European Journal of Radiology Open 11 (2023) 100535

Contents lists available at ScienceDirect

European Journal of Radiology Open

journal homepage: www.elsevier.com/locate/ejro

Assessment of LI-RADS efficacy in classification of hepatocellular carcinoma and benign liver nodules using DCE-MRI features and machine learning

Maryam Fotouhi [a], Fardin Samadi Khoshe Mehr [b], Sina Delazar [a], Ramin Shahidi [c], Babak Setayeshpour [d], Mohssen Nassiri Toosi [e], Arvin Arian [a,*]

[a] Advanced Diagnostic and Interventional Radiology (ADIR), Radiology department, Imam Khomeini Hospital Complex, Tehran University of Medical Science, Iran
[b] Research Centre for Molecular and Cellular Imaging (RCMCI), Advanced Medical Technologies and Equipment Institute (AMTEI), Tehran University of Medical Sciences, Tehran, Iran
[c] School of Medicine, Bushehr University of Medical Sciences, Bushehr, Iran
[d] Erfan Niayesh hospital, Radiology department, Tehran, Iran
[e] Imam Khomeini Hospital Complex, Liver Transplantation Research Centre, Tehran University of Medical Sciences, Tehran, Iran

ARTICLE INFO

Keywords:
LI-RADS
Machine learning
Hepatocellular carcinoma
Dynamic contrast-enhanced MRI
Cirrhotic nodule

ABSTRACT

Purpose: The current study aimed to evaluate the efficiency of dynamic contrast-enhanced (DCE) MRI visual features in classifying benign liver nodules and hepatocellular carcinoma (HCC) using a machine learning model.
Methods: 115 LI-RADS3, 137 LI-RADS4, and 140 LI-RADS5 nodules were included (392 nodules from 245 patients), which were evaluated by follow-up imaging for LR-3 and pathology results for LR-4 and LR-5 nodules. Data was collected retrospectively from 3 T and 1.5 T MRI scanners. All the lesions were categorized into 124 benign and 268 HCC lesions. Visual features included tumor size, arterial-phase hyper-enhancement (APHE), washout, lesion segment, mass/mass-like, and capsule presence. Gini-importance method extracted the most important features to prevent over-fitting. Final dataset was split into training(70%), validation(10%), and test dataset(20%). The SVM model was used to train the classifying algorithm. For model validation, 5-fold cross-validation was utilized, and the test data set was used to assess the final accuracy. The area under the curve and receiver operating characteristic curves were used to assess the performance of the classifier model.
Results: For test dataset, the accuracy, sensitivity, and specificity values for classifying benign and HCC lesions were 82%,84%, and 81%, respectively. APHE, washout, tumor size, and mass/mass-like features significantly differentiated benign and HCC lesions with p-value $< .001$.
Conclusions: The developed classification model employing DCE-MRI features showed significant performance of visual features in classifying benign and HCC lesions. Our study also highlighted the significance of mass and mass-like features in addition to LI-RADS categorization. For future work, this study suggests developing a deep-learning algorithm for automatic lesion segmentation and feature assessment to reduce lesion categorization errors.

1. Introduction

The sixth most common type of cancer worldwide is hepatocellular carcinoma (HCC), which accounts for 75% of all liver tumors [1]. As one-third of patients with chronic liver cirrhosis develop the disease at some point in their lives, they are at high risk for developing hepatocellular carcinoma [2]. Early detection and accurate diagnosis are crucial for effective treatment and improved patient outcomes. Liver

Abbreviations: **HCC**, Hepatocellular carcinoma; **LI-RADS**, Liver Imaging Reporting and Data System; **CE-MRI**, Contrast-enhanced MRI; **SPGR**, Spoiled gradient-recalled echo; **SSFSE**, Single-shot fast spin echo; **DWI**, Diffusion-weighted imaging; **DCE**, Dynamic contrast-enhanced; **EPI**, Echo planar imaging; **APHE**, Arterial phase hyperenhancement; **SMOTE**, Synthetic Minority Oversampling Technique; **AUC**, Area under the curve; **ROC**, Receiver operating characteristics.

* Correspondence to: Advanced Diagnostic and Interventional Radiology (ADIR), Cancer Institute, Radiology Department, Imam Khomeini Hospital Complex, Tehran University of Medical Science, Qarib St, Keshavarz Blvd, Tehran 14194, Iran.
E-mail address: aryana@sina.tums.ac.ir (A. Arian).

https://doi.org/10.1016/j.ejro.2023.100535
Received 21 May 2023; Received in revised form 12 October 2023; Accepted 23 October 2023

Imaging Reporting and Data System (LI-RADS) was developed by the American College of Radiology to standardize the interpretation and reporting of liver imaging studies, particularly for patients at high risk for hepatocellular carcinoma (HCC). A liver lesion in a high-risk patient (cirrhosis, chronic HBV infection, current or prior HCC) is assigned LI-RADS (LR) category, indicating the possibility of acquiring HCC, ranging from LR-1 to LR-5. LR-1 and LR-2 are definitely and probably benign; LR-3 indicates a moderate risk of HCC, LR-4 is a high risk without certainty, and LR-5 is definitely HCC [3,4].

Based on meta-analyses and expert consensus, multiphase contrast-enhanced MRI (CE-MRI) coupled with intravenous gadoxetate disodium achieves an 80% staging accuracy in diagnosis with the more accurate and radiation-free diagnosis of HCC [5–8]. DCE-MRI, as a powerful imaging modality, can provide detailed information about the vascular characteristics of liver nodules. Besides, LI-RADS liver lesion score on CE-MRI includes assessing tumor size, arterial phase non-rim hyperenhancement (APHE), washout, threshold growth, and capsule presence [9]. Visual assessment of liver nodules in cirrhotic patients is a major part of international guidelines for the treatment of liver nodules [10]. The concept of accuracy for main feature characterization and for LR-5 category assignment is fundamental to LI-RADS and aims to reduce discrepancies across radiologists. However, some margin for error remains due to interreader variability in each characteristic, which could be amplified if a large number of characteristics or longitudinal data were used. Size measurement and APHE detection are the areas where interreader consistency is greatest, but it is less effective for washout and enhancing capsule [11].

The performance of LI-RADS was evaluated using visual features in MRI sequences, including T1, T2-weighted, and CE-perfusion [12,13]. In V. Granta's study, the results demonstrated the high performance of LI-RADS in classifying benign and malignant lesions with a sensitivity of 100%, a specificity of 81.3%, and an accuracy of 96.3% [14]. Another study published in 2021 by Zhong et al.[15] evaluated the performance of LI-RADS in a cohort of 150 patients with liver nodules who underwent T1W, T2W, and ADC-MRI. The authors compared the diagnostic accuracy of LI-RADS to radiomics features in combination with linear regression classifier. The designed model showed a higher classification performance compared with LI-RADS alone (area under curve (AUC) = 0.91 vs 0.89).

Recently, an improvement in classification accuracy with multiple features can be achieved through machine learning. As reported previously, deep learning and machine learning classifiers can differentiate between LR-3 and LR-4,5 by utilizing clinical and image-extracted features [16–19]. This breakthrough, combined with the functional features derived from vascular perfusion patterns, has remarkable potential to open up new possibilities for predicting early pathology/follow-up results for HCC patients.

To the best of our knowledge, no previous research has used visual features from MRI-DCE to train machine learning algorithms to assist radiologists in primary diagnosis. Thus, this study aims to explore the potential of LI-RADS in conjunction with machine learning techniques to diagnose HCC in cirrhotic patients with high accuracy. We tested this idea using visual DCE-MRI features and the SVM classifier.

2. Material and methods

2.1. Patients

This retrospective study was approved by the university review board, and the requirement for written informed consent was waived. All patients were discussed at the regional reference center at the time of image acquisition, and its tumor board in "… name of the center …" was screened between April 2019 and December 2022. For data inclusion and evaluation in this study, an expert radiologist with eight years of expertise conducted a comprehensive evaluation on cirrhotic patients without vascular abnormalities. The findings were subsequently reviewed and confirmed by a diagnostic radiologist with 11 years of experience. Lesions falling within the LI-RADS 3–5 category were carefully examined and subsequently classified, ensuring that prior reports were not taken into consideration during the assessment process. A total of 245 patients with 392 nodules met the inclusion criteria (Fig. 1): (i) 140 LR-5 definitely HCC nodules, which were evaluated by post-operative sample pathology results; (ii) 115 LR-3 intermediate probability of malignancy liver nodules, which were evaluated by last follow-up imaging; (iii) 137 LR-4 the probably HCC nodules, which were evaluated by core needle biopsy and pathology results. We divided all nodules into two cohorts: 1- benign nodules (124 nodules; 113 nodules from LR-3 and 11 nodules from LR-4) 2- HCC nodules (268 nodules; 140 nodules from LR-5, 126 nodules from LR-4, and 2 nodules from LR-3).

2.2. MRI imaging acquisition

MRI was performed using a 3 T (GE Medical Systems, Discovery 750w) and external test set in 1.5 T (GE Medical System, Signa) MRI scanners. To assess the effectiveness of the model created using 3 T MRI data (193 patients with 314 lesions), the combination dataset of patients who underwent imaging with a 1.5 T (30 patients with 42 lesions) and 3 T (22 patients with 36 lesions) MRI scanner were utilized as an external test dataset. The regular procedures and techniques included the following: 1) DCE-MRI, LAVA sequence, based on a 3D spoiled gradient-recalled echo (SPGR) sequence with uniform fat suppression, was conducted in the axial plane with a breath-hold 2D gradient echo T1-weighted sequence. The baseline signal intensity was acquired 10 s before the contrast agent's injection (Gadolinium-diethylene triamine pentaacetate, GD-DTPA, 0.1 mmol/kg body weight, a flow rate of 2.0 ml/s). Thirty-six dynamic contrast slices with a temporal resolution of 4 s/image were acquired during 66 acquisition phases and normal breathing. 2) Axial T2 -weighted with single-shot fast spin echo (SSFSE) sequence. 3) Before contrast agent injection, diffusion-weighted imaging (DWI) with three orthogonal orientations and respiratory-triggered 2D echo planar imaging (EPI) with three b-values (0, 200, 800 s/mm2) were performed. Table 1 provides details on image acquisition parameters.

2.3. Visual feature assessment and segmentation

Following the process of inclusion categorization, subsequent to a distinct time interval, visual characteristics were evaluated by a radiologist with eight years of experience in the field and subsequently verified by another radiologist with 11 years of expertise in diagnostic radiology. Visual characteristics of non-rim arterial phase hyperenhancement (APHE), enhancing capsule, non-peripheral washout, and tumor size were evaluated according to standard definitions. Another important characteristic that was evaluated beyond the main features of LIRADS criteria is the mass and mass-like configuration, which refers to a discrete lesion that is distinct from the surrounding liver tissue. Any

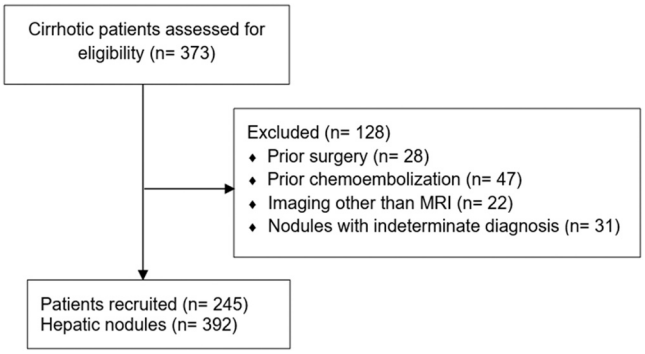

Fig. 1. Inclusion and study population.

Table 1
MR Imaging parameters in 1.5 T and 3 T scanners.

Sequence	Repetition time (ms)	Echo time (ms)	Inversion time (ms)	Slice thickness (mm)	Flip angle	B value (s/mm^2)
T1WI	100	4.2	120	5	24°	-
T2WI	538	110	150	5	90°	-
DWI	9400	70	110	8	90°	0, 200, 800
DCE	3.7	1.7	5	5	15°	-

MRI: Magnetic resonance imaging, T1WI: T1-weighted imaging, T2WI: T2-weighted imaging, DWI: Diffusion-weighted imaging, DCE: Dynamic contrast-enhanced.

three-dimensional space-occupying observation displaces or distorts background hepatic parenchyma, such as an expansile, infiltrative, or tumoral mass in the vein, is considered a mass-like configuration [4]. Fig. 2 displays illustrative sequences in explanation for a 65-year-old patient with HCC diagnosis with assessing the visual features.

2.4. Data splitting and balancing

For the robustness and generalizability of our model, we split our dataset into three subsets: a training set for model training (70%), a validation set (10%) for hyperparameters tuning and model selection using 5-fold cross-validation, and a final external dataset (20%) for evaluating the performance of the selected model on unseen data. All the data of the 1.5 T MRI dataset were used for testing and not used in the training process. Table 2 provides details on splitting of training/validation and test datasets. Unbalancing effect between benign and HCC lesions was minimized by utilizing the Synthetic Minority Oversampling Technique (SMOTE) to avoid insufficient training and inaccurate prediction since our study's predominant diagnosis is HCC (69% vs. 31%) [20].

Table 2
Data splitting- training/validation and test datasets.

Dataset	*Pathology*		*MRI scanner*	
	BENIGN	*HCC*	*1.5 T*	*3 T*
*Training/Validation**	92	222	0	314 (193 patients)
*Test**	32	46	42 (30 patients)	36 (22 patients)

*Number of lesions

2.5. Classification model construction

The most significant features were chosen using the Gini importance technique to avoid overfitting. The classification model was trained using four features with a Gini importance rate exceeding 0.2. The Gini importance quantifies how much each feature contributes to decreasing impurity in a dataset, helping decision tree algorithm identify and select features that are most effective at splitting and organizing data. We implemented the classification algorithm in open-source Scikit-learn API in Python software [21]. We used Support Vector Machine (SVM) as the classifier for classification method. The SVM setting involved several parameters that were optimized to achieve the best performance. The first parameter was the kernel function, which determined how the data is transformed into a higher-dimensional space for classification. In this study, we used the radial basis function kernel, which is commonly used in SVM classification. The second parameter was the regularization parameter C, which controls the trade-off between maximizing misclassifications. We used a grid search approach to find the optimal C value that maximizes accuracy. The third parameter was gamma, which determines how far the influence of a single training example reaches. A small gamma means that only nearby points are considered for classification, while a large gamma means that more distant points are also considered. Our study used the grid search approach to find the optimal

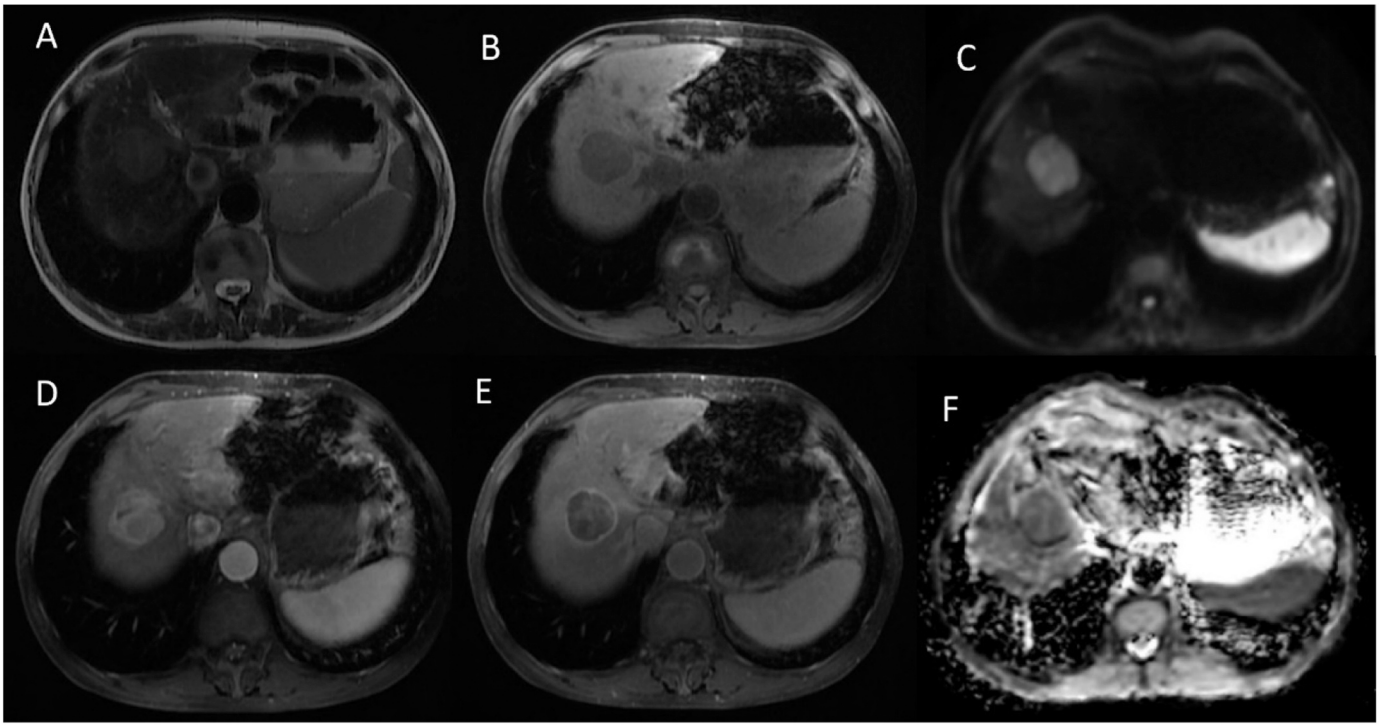

Fig. 2. Hepatocellular carcinoma in a 65-year-old man. A. Axial T2-weighted imaging shows a 40 × 35 mm mass with mild-moderate high signal intensity in segment VIII, B. In-phase T1-weighted depicts a low signal intensity C. Diffusion-weighted imaging (DWI) with b-value:1000 with restriction, D. Arterial phase postcontrast T1 fat-suppressed (FS) with arterial phase hyperenhancement, E. Venous phase postcontrast T1 FS depicts washout, F. Apparent diffusion coefficient (ADC) map with decreased signal comparing to background liver.

value of gamma to maximize accuracy.

Finally, cross-validation was used to evaluate and compare different SVM settings. 5-fold cross-validation was used to estimate the generalization performance of each setting and select the best one. In addition to cross-validation on the training set, a calibration set was used to prevent overfitting. The AUC was calculated for candidate models generated based on the training set and also the performance of the candidate model was evaluated by checking the AUC on an external dataset comprising of both 1.5 T and 3 T MRI datasets. Fig. 3 depicts the analytical process of feature extraction and selection, model construction, validation, and final performance test. To determine the correlation between visual features and benign or HCC tumors, Spearman's correlation was applied. Fisher's exact test or $\mathcal{X}2$ was used to compare categorical variables. The T-test was used to compare continuous variables.

3. Results

3.1. Clinical characteristics

Two hundred forty-five participants (109 males; mean age 59.08 ± 14.53; range 29–72) with 392 lesions (mean size 28.45 ± 33.17 mm) from LI-RADS 3–5 were divided into benign and HCC groups based on their pathology or follow-up results. A total of 268 HCC tumors and 124 benign lesions were identified. APHE was present in 72% of cases in HCC tumors, whereas in benign masses, it was only present in 18.5% of cases. Mass configuration was present in 86.6% of HCC and mass-like in 26.6% of benign lesions ($P < 0.001$). Non-peripheral washout appearance was recorded by 84.7% in HCC and 11.2% in benign lesions ($P < 0.001$). Clinical features and visual assessment of the included lesions are shown in Table 3. The regression analysis results indicated a significant positive correlation between mass/mass-like, APHE, and washout and benign/HCC groups with $R2 = 0.83$ and $P < 0.001$, $R2 = 0.65$ and $P < 0.001$, and $R2 = 0.8$ and $P < 0.001$, respectively (Table 3).

Table 3
Clinical characteristics.

Parameters	Benign (n = 124)	HCC (n = 268)	P-value	Correlation value
LI-RADS 3	**113**	**2**	-	-
LI-RADS 4	**11**	**126**	-	-
LI-RADS 5	**0**	**140**	-	-
Age	63.2.4 ± 10.2	69.2 ± 13.5	0.52	0.06
Sex (M/F)	35/49	74/87	0.73	0.07
Tumor Size (mm)	8.9 ± 3.1	28.9 ± 16.4	**0.002** *	0.32
Mass/Mass-like	33/91	233/36	**< 0.001***	0.79
APHE (Yes/No)	23/101	193/75	**< 0.001** *	0.62
Capsule (Yes/No)	52/72	161/107	0.6	0.03
Washout (Yes/No)	14/110	227/41	< 0.001 *	0.86

Arterial phase hyperenhancement: APHE, Hepatocellular Carcinoma: HCC

3.2. Machine learning

The Gini importance rate threshold for benign and hepatocellular carcinoma (HCC) tumors was set at 0.2, and the corresponding Gini importance values for the features are presented in Table 4. Among the selected features, mass/mass-like, Washout, Tumor Size, and APHE exhibited importance rates of 2.8, 2.4, 2.1, and 2, respectively. Notably,

Table 4
Importance rate of features using GINI-random forest.

Features	Importance rate
mass	0.28
Washout	0.24
Tumor Size	0.21
APHE	0.2
Capsule	0.06
Segment	0.03
Age	0.01

Arterial phase hyperenhancement: APHE

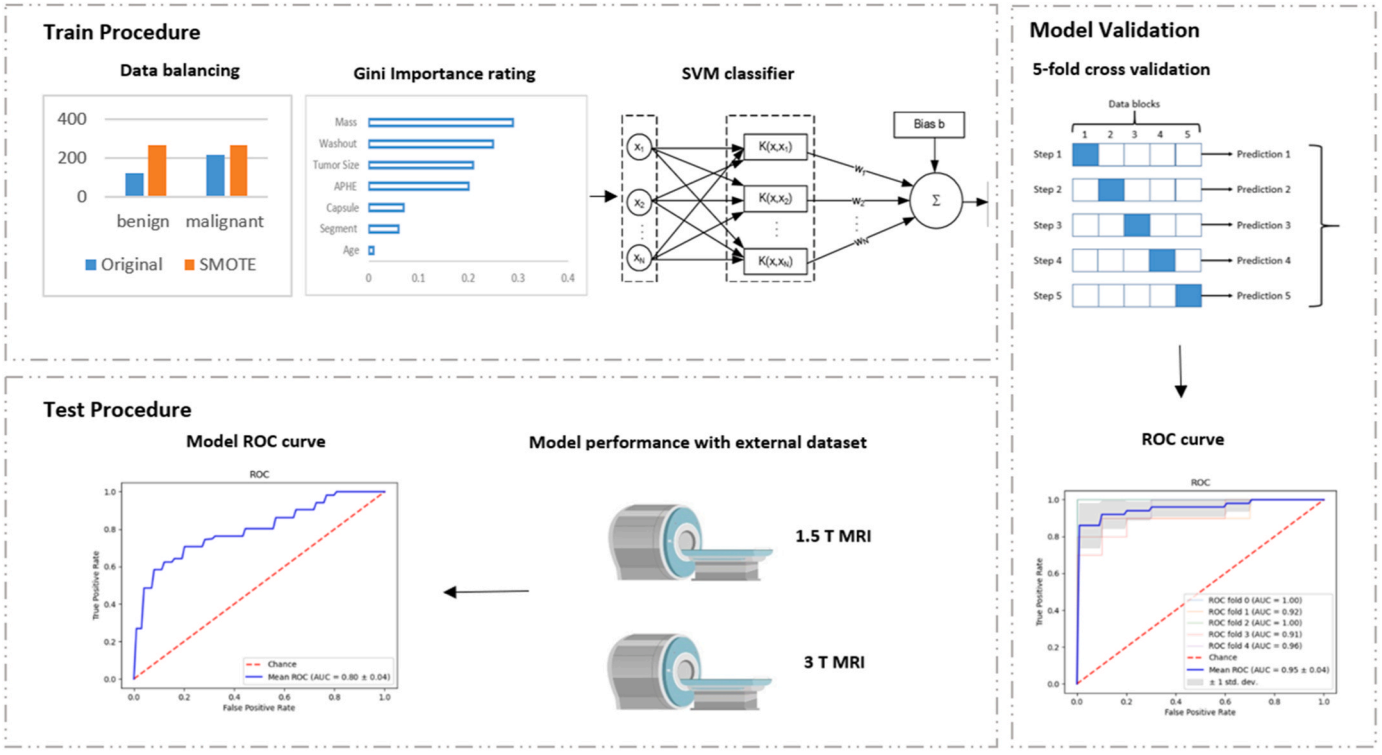

Fig. 3. Study workflow. Training procedure: Qualitative features, GINI importance feature reduction, Synthetic Minority Oversampling Technique (SMOTE) based data balancing, SVM, and 5-fold cross-validation. Test procedure and receiver operating characteristics (ROC).

the mass/mass-like feature demonstrated the highest importance rate, underscoring its paramount significance in the classification task. The sample size for benign and HCC cases was the same at 222 after data balancing using the SMOTE approach, as shown in Fig. 1. Regarding accuracy, precision, recall, and F1-score, the SVM classifier with the training dataset achieved 100%, 1.00, 1.00, 1.00, and 1.00. The result indicates that our model could accurately classify all of the data points in our dataset. To further validate our SVM model, the model was subsequently tested on the same 3 T scans as well as the external set from 1.5 T dataset. The results from testing our SVM model on the external dataset were promising, with an accuracy of 82%, sensitivity of 0.84, specificity of 0.81, recall of 0.8, and F1-score of 0.82. These results suggest our SVM model robustness and can generalizability. Fig. 4 illustrates how visual features extracted from DCE-MRI were used to distinguish benign liver nodules from HCC to achieve an AUC in receiver operating characteristics (ROC) of 1 in the validation step and AUC of 0.8 in the final test step.

4. Discussion

The accurate classification of liver nodules as benign and HCC is crucial for effective management strategies, as surveillance or biopsy. LI-RADS has been developed to standardize the reporting and management of liver nodules detected in imaging studies, including DCE-MRI [22]. However, the accuracy of LI-RADS in distinguishing between benign and HCC nodules can be challenging, particularly in case where there is uncertainty or disagreement among radiologists. There have been some errors associated with the ability to correctly classify LR-3, LR-4, and LR-5 categories using this method. Following up on LR-3 cases requires repeating imaging twice annually until a definitive diagnosis is made, whereas most LR-4 subjects require a biopsy [23]. Therefore, this approach needs to be evaluated to determine whether it is accurate in predicting the type of tumor without contributing to artificial errors.

SVM is preferred over other classifiers due to its effectiveness in high-dimensional spaces, good generalization performance, robustness to noise, ability to handle non-linearly separable data, efficiency, and tunability [24]. This study aimed to assess the effectiveness of LI-RADS in classifying liver nodules through the use of DCE-MRI visual features and machine learning. Our findings revealed a 100% accuracy rate with the training dataset using cross-validation and an 82% accuracy rate with an external dataset. These results suggest that visual features, including LI-RADS, could offer a non-invasive and precise approach for detecting and managing liver cancer. Notably, our study also highlighted the significance of mass and mass-like features in addition to LI-RADS categorization, which were not considered as major features compared to other features but were found to be among the important features based on the Gini importance rating method. It has been demonstrated that LI-RADS criteria can predict HCC with considerable accuracy, which is accessible to expert radiologists. Recent studies have shown that by correctly evaluating the visual features of liver nodules using the LI-RADS criteria, an expert radiologist can predict HCC with considerable accuracy. However, with the potential of computational algorithms, automating these steps can significantly improve the accuracy and efficacy of LI-RADS in clinical settings.

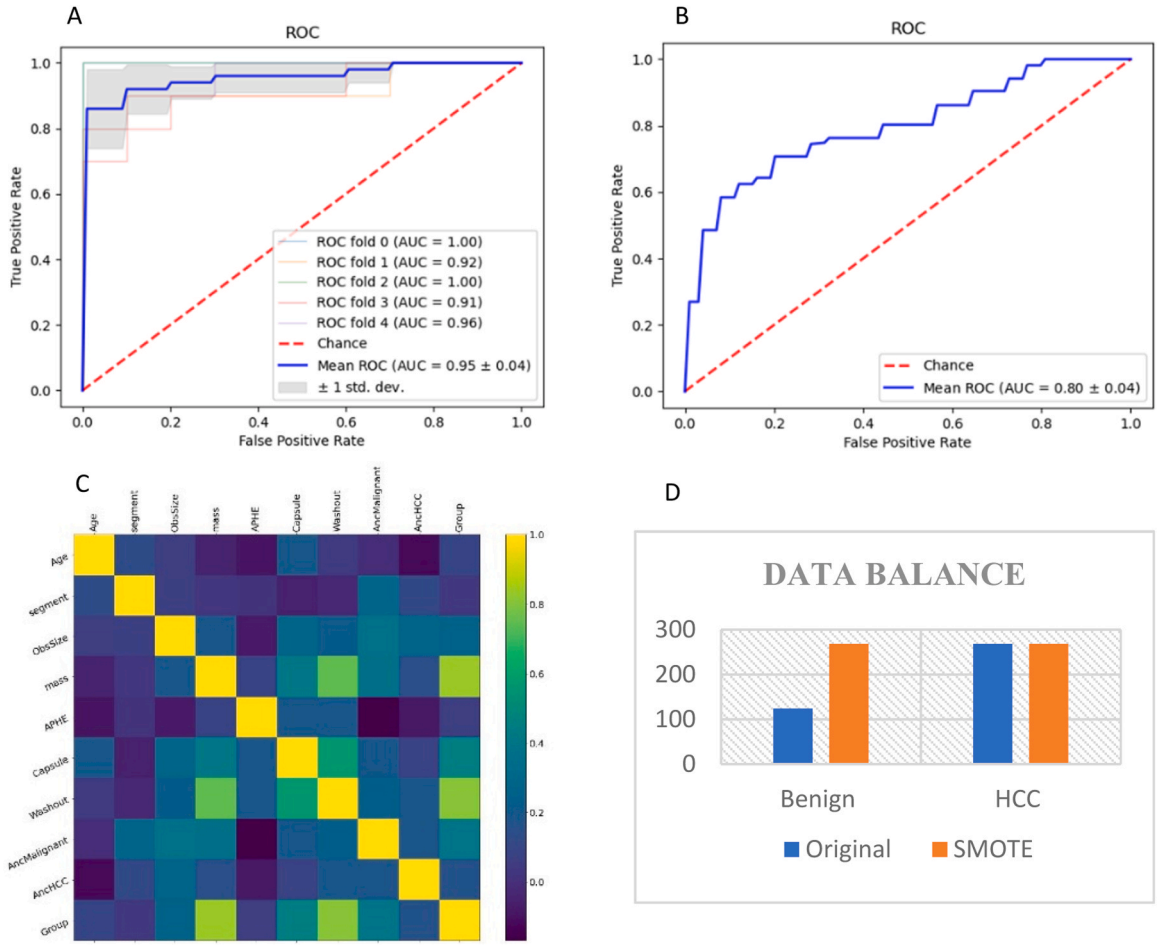

Fig. 4. A. SVM validation ROC curve B. ROC curve of model on the test dataset to predict pathology result using LIRADS-based qualitative features extracted from dynamic contract enhanced (DCE)-MRI C. Synthetic Minority Oversampling Techniques (SMOTE) based data balancing result D. Correlation map between qualitative features and groups.

The LI-RADS features methodology was evaluated by Granta et al. (2022) for the classification of benign and HCC lesions. Their results indicate high accuracy, sensitivity, and specificity with 96%, 100%, and 81.3%, respectively [14]. The development of machine-learning models for predicting pathology in cancers, such as HCC, which are trained with quantitative characteristics derived from MRI with/without radiomics, has been a hotbed of research [25]. In 2021, Starmans et al. developed a machine-learning model based on radiomics to distinguish benign from HCC lesions based on T2-weighted MRI. They achieved an accuracy of 78% in the internal validation of the dataset and a similar AUC in the external validation [26]. Some studies use MRI imaging to classify liver lesions as benign or HCC by employing deep learning algorithms. The U-net is used to differentiate HCC lesions from non-HCC lesions in a study by Oestmann et al. (2021). Accordingly, their accuracy, sensitivity, and specificity were 87.3%, 92.7%, and 82%, respectively [27]. In Yuan Wu's (2020) study, the AlexNet convolutional neural network was trained using CE-MRI images labeled by radiologists to distinguish LR-3 and LR-4,5. Their results achieved a high accuracy of 0.9, a sensitivity of 1, a precision of 0.835, and an area-under-curve (AUC) of 0.95, referencing the expert human radiologist report [28]. Mokrane et al. (2019) developed machine-learning algorithms using radiomics features and pathology-proven CT datasets to diagnose HCC in intermediate-risk liver nodules. Their results showed an accuracy of 0.8 for predicting pathology response using CT and radiomics-driven features [19]. In a recent study conducted by Yang Xu et al. (2023), a deep learning algorithm was trained to automatically classify liver lesions in LR3-LR5 classes. The findings revealed that the model achieved an accuracy rate of 83%, slightly lower than the 86% accuracy rate achieved by radiologists. This suggests that LIRADS-based features have the potential for use in decision-making models when compared to deep-based features. Additionally, they trained their model to differentiate between hepatocellular carcinoma (HCC) and non-HCC lesions, achieving a test validation accuracy of 86.5% and an external validation accuracy of 71.5%. It is worth noting that CT images were utilized for training the model, resulting in lower accuracy compared to models trained using MRI images, particularly DCE-MRI images [29].

Our study has several limitations. First, the size of our train/test sample was not very large compared to those of big databases, which may have impacted the generalizability of our findings. In order to mitigate the impact of this effect, we tested the generalizability of the technique by using an external dataset obtained from a different MRI unit. Second, when constructing our model, we relied solely on DCE MRI visual characteristics; however, alternative sequences can be included to conduct further tests and evaluate the model's resilience. In further research, it may be possible to investigate the efficacy of further merging various imaging modalities, such as diffusion-weighted imaging, in an effort to achieve higher rates of diagnostic precision. One additional constraint of this study pertained to the unavailability of pathology results for patients initially classified in the LR-3 category but subsequently reclassified as LR-4 or LR-5 during 6–12 month follow-up and awaiting biopsy. By obtaining access to the longitudinal data for these patients, it would be possible to develop predictive models capable of forecasting pathology results during the early stage.

5. Conclusion

Our study demonstrates that machine learning algorithms can accurately predict HCC using LI-RADS visual features assessed on DCE-MRI. Our study also highlighted the significance of mass and mass-like features in addition to LI-RADS categorization. Despite its good performance on training data, it was not sufficiently powered to pick up significant difference patterns in the new test dataset. However, it was the most important feature to recognize the optimal pattern for the HCC prediction. These findings should be interpreted with caution given the several limitations of this study, but they encourage future studies to investigate new optimal features with higher importance rates to enhance the robustness and generalizability of decision-making models. Deep learning/radiomics-based features will be crucial for future studies to improve accuracy.

Funding

This research did not receive any specific grant from funding agencies in the public, commercial, or not-for-profit sectors. Acknowledgment. Thanks to all who helped us with this project.

Ethical statement

This study was performed in line with the principles of the Declaration of Helsinki. Approval was granted by the Tehran University of Medical Sciences research ethics committee. The authors have no relevant financial or non-financial interests to disclose.

CRediT authorship contribution statement

Delazar Sina: Writing – review & editing. **Shahidi Ramin:** Investigation, Conceptualization. **Fotouhi Maryam:** Writing – review & editing, Writing – original draft, Project administration. **Samadi Khoshe Mehr Fardin:** Writing – original draft, Software, Investigation. **Arian Arvin:** Writing – review & editing, Supervision, Methodology. **Setayeshpour Babak:** Supervision, Resources, Methodology. **Nassiri Toosi Mohssen:** Writing – review & editing, Data curation, Conceptualization.

Declaration of Competing Interest

The authors declare no conflict of interest.

References

[1] K.A. McGlynn, J.L. Petrick, H.B. El-Serag, Epidemiology of hepatocellular carcinoma, Hepatology 73 (Suppl 1) (2021) 4–13.
[2] D. Tümen, P. Heumann, K. Gülow, C.N. Demirci, L.S. Cosma, M. Müller, A. Kandulski, Pathogenesis and current treatment strategies of hepatocellular carcinoma, Biomedicines 10 (12) (2022).
[3] K.M. Elsayes, A.Z. Kielar, V. Chernyak, A. Morshid, A. Furlan, W.R. Masch, R. M. Marks, et al., LI-RADS: a conceptual and historical review from its beginning to its recent integration into AASLD clinical practice guidance, J. Hepatocell. Carcinoma 6 (2019) 49–69.
[4] K.M. Elsayes, A.Z. Kielar, M.M. Agrons, J. Szklaruk, A. Tang, M.R. Bashir, D. G. Mitchell, et al., Liver Imaging Reporting and Data System: an expert consensus statement, J. Hepatocell. Carcinoma 4 (2017) 29–39.
[5] Y. Liang, F. Xu, Y. Guo, L. Lai, X. Jiang, X. Wei, H. Wu, et al., Diagnostic performance of LI-RADS for MRI and CT detection of HCC: A systematic review and diagnostic meta-analysis, Eur. J. Radiol. 134 (2021), 109404.
[6] J. Shin, S. Lee, J.K. Yoon, Y.E. Chung, J.Y. Choi, M.S. Park, LI-RADS major features on MRI for diagnosing hepatocellular carcinoma: a systematic review and meta-analysis, J. Magn. Reson. Imaging 54 (2) (2021) 518–525.
[7] C.B. van der Pol, M.D. McInnes, J.P. Salameh, B. Levis, V. Chernyak, C.B. Sirlin, M. R. Bashir, et al., CT/MRI and CEUS LI-RADS major features association with hepatocellular carcinoma: individual patient data meta-analysis, Radiology 302 (2) (2022) 326–335.
[8] A. Esposito, V. Buscarino, D. Raciti, E. Casiraghi, M. Manini, P. Biondetti, L. Forzenigo, Characterization of liver nodules in patients with chronic liver disease by MRI: performance of the Liver Imaging Reporting and Data System (LI-RADS v.2018) scale and its comparison with the Likert scale, Radiol. Med. 125 (1) (2020) 15–23.
[9] V. Granata, R. Fusco, A. Avallone, O. Catalano, F. Filice, M. Leongito, R. Palaia, et al., Major and ancillary magnetic resonance features of LI-RADS to assess HCC: an overview and update, Infect. Agent. Cancer 12 (2017), 23.
[10] J. Gregory, M. Dioguardi Burgio, G. Corrias, V. Vilgrain, M. Ronot, Evaluation of liver tumour response by imaging, JHEP Rep. 2 (3) (2020), 100100.
[11] V. Granata, R. Fusco, S.V. Setola, C. Picone, P. Vallone, A. Belli, P. Incollingo, et al., Microvascular invasion and grading in hepatocellular carcinoma: correlation with major and ancillary features according to LIRADS, Abdom. Radiol. (NY) 44 (8) (2019) 2788–2800.
[12] A. Arian, A.D. Abdullah, H.J. Taher, H.S. Alareer, M. Fotouhi, Diagnostic values of the liver imaging reporting and data system in the detection and characterization of hepatocellular carcinoma: a systematic review and meta-analysis, Cureus 15 (3) (2023).

[13] M.E. Laino, L. Viganò, A. Ammirabile, L. Lofino, E. Generali, M. Francone, A. Lleo, et al., The added value of artificial intelligence to LI-RADS categorization: a systematic review, Eur. J. Radiol. (2022), 110251.
[14] V. Granata, R. Fusco, S. Venanzio Setola, M.L. Barretta, D.M.A. Iasevoli, R. Palaia, A. Belli, et al., Diagnostic performance of LI-RADS in adult patients with rare hepatic tumors, Eur. Rev. Med. Pharmacol. Sci. 26 (2) (2022) 399–414.
[15] X. Zhong, T. Guan, D. Tang, J. Li, B. Lu, S. Cui, H. Tang, Differentiation of small (≤ 3 cm) hepatocellular carcinomas from benign nodules in cirrhotic liver: the added additive value of MRI-based radiomics analysis to LI-RADS version 2018 algorithm, BMC Gastroenterol. 21 (1) (2021) 1–10.
[16] V. Granata, R. Fusco, F. De Muzio, C. Cutolo, S.V. Setola, F. Dell'Aversana, F. Grassi, et al., Radiomics and machine learning analysis based on magnetic resonance imaging in the assessment of liver mucinous colorectal metastases, Radiol. Med. 127 (7) (2022) 763–772.
[17] A. Alksas, M. Shehata, G.A. Saleh, A. Shaffie, A. Soliman, M. Ghazal, A. Khelifi, et al., A novel computer-aided diagnostic system for accurate detection and grading of liver tumors, Sci. Rep. 11 (1) (2021), 13148.
[18] M.E. Laino, L. Viganò, A. Ammirabile, L. Lofino, E. Generali, M. Francone, A. Lleo, et al., The added value of artificial intelligence to LI-RADS categorization: A systematic review, Eur. J. Radiol. 150 (2022), 110251.
[19] F.Z. Mokrane, L. Lu, A. Vavasseur, P. Otal, J.M. Peron, L. Luk, H. Yang, et al., Radiomics machine-learning signature for diagnosis of hepatocellular carcinoma in cirrhotic patients with indeterminate liver nodules, Eur. Radiol. 30 (1) (2020) 558–570.
[20] J. Li, Q. Zhu, Q. Wu, Z. Fan, A novel oversampling technique for class-imbalanced learning based on SMOTE and natural neighbors, Inf. Sci. 565 (2021) 438–455.
[21] F. Pedregosa, G. Varoquaux, A. Gramfort, V. Michel, B. Thirion, O. Grisel, M. Blondel, et al., Scikit-learn: machine learning in Python, J. Mach. Learn. Res 12 (2011) 2825–2830.
[22] S.K. Rodgers, D.T. Fetzer, H. Gabriel, J.H. Seow, H.H. Choi, K.E. Maturen, A. P. Wasnik, et al., Role of US LI-RADS in the LI-RADS Algorithm, Radiographics 39 (3) (2019) 690–708.
[23] K.M. Elsayes, K.J. Fowler, V. Chernyak, M.M. Elmohr, A.Z. Kielar, E. Hecht, M. R. Bashir, et al., User and system pitfalls in liver imaging with LI-RADS, J. Magn. Reson. Imaging 50 (6) (2019) 1673–1686.
[24] D.A. Pisner, D.M. Schnyer, Support vector machine. in: S.V. Andrea Mechelli (Ed.), Machine learning, Elsevier, Academic Press,, 2020, pp. 101–121.
[25] H. Jiang, X. Liu, J. Chen, Y. Wei, J.M. Lee, L. Cao, Y. Wu, et al., Man or machine? prospective comparison of the version 2018 EASL, LI-RADS criteria and a radiomics model to diagnose hepatocellular carcinoma, Cancer Imaging 19 (1) (2019), 84.
[26] M.P. Starmans, R.L. Miclea, V. Vilgrain, M. Ronot, Y. Purcell, J. Verbeek, W. J. Niessen, et al., Automated differentiation of malignant and benign primary solid liver lesions on MRI: an externally validated radiomics model, medRxiv 2021 (2021), 08. 10.21261827.
[27] P.M. Oestmann, C.J. Wang, L.J. Savic, C.A. Hamm, S. Stark, I. Schobert, B. Gebauer, et al., Deep learning–assisted differentiation of pathologically proven atypical and typical hepatocellular carcinoma (HCC) versus non-HCC on contrast-enhanced MRI of the liver, Eur. Radiol. 31 (7) (2021) 4981–4990.
[28] Y. Wu, G.M. White, T. Cornelius, I. Gowdar, M.H. Ansari, M.P. Supanich, J. Deng, Deep learning LI-RADS grading system based on contrast enhanced multiphase MRI for differentiation between LR-3 and LR-4/LR-5 liver tumors, Ann. Transl. Med. 8 (11) (2020) 701.
[29] Y. Xu, C. Zhou, X. He, R. Song, Y. Liu, H. Zhang, Y. Wang, et al., Deep learning–assisted LI-RADS grading and distinguishing hepatocellular carcinoma (HCC) from non-HCC based on multiphase CT: a two-center study, Eur. Radiol. (2023) 1–10.